

Neon Matrix Infrared Spectrum of WH_6 : A Distorted Trigonal Prism Structure

Xuefeng Wang and Lester Andrews*

Department of Chemistry, University of Virginia, P.O. Box 400319, Charlottesville, Virginia 22904-4319

Received February 11, 2002

Valence shell electron pair repulsion (VSEPR) theory occupies a central position in structural chemistry, and it has enjoyed much predictive success.¹ One exception is for octahedral symmetry, which is predominant in transition-metal chemistry, but CrH_6 and WH_6 hexahydrides are computed to have lower symmetry-distorted trigonal prismatic structures.^{2–6} In fact the stabilization for WH_6 is substantial: the C_{3v} prism is well over 100 kcal/mol more stable than the octahedral form, depending on the calculation.^{3–6} Although no experimental data are available for WH_6 , the closely related $\text{W}(\text{CH}_3)_6$ molecule has the distorted prismatic structure with three-fold symmetry based on gas-phase electron diffraction and low-temperature single-crystal X-ray diffraction investigations.^{7,8} Ab initio and density functional theoretical calculations show that the equilibrium structure of $\text{W}(\text{CH}_3)_6$ has local C_{3v} symmetry for the WC_6 skeleton,⁶ which is the same structure proposed by theory for WH_6 .^{3–6} The infrared spectrum is sensitive to symmetry, and thus observation of the infrared spectrum of WH_6 could in principle determine the WH_6 structure.

Ongoing investigations of reactions of laser-ablated metal atoms with H_2 in condensing noble gases have found several systems where the initial hydrides formed react with additional H_2 to produce higher hydrides or higher dihydrogen complexes. Examples include TiH_4 , HfH_4 , $(\text{H}_2)\text{AuH}$, and $(\text{H}_2)\text{RhH}_2$.^{9–12} We apply this method to the synthesis of WH_6 , and we show that the infrared spectrum containing four W–H stretching modes (two a_1 and two e) matches frequencies computed by density functional theory (DFT) for the distorted prismatic C_{3v} structure.

The experiment for reactions of laser-ablated metal atoms with small molecules during condensation in excess neon has been described previously.^{11–15} The Nd:YAG laser fundamental (1064 nm, 10 Hz repetition rate with 10 ns pulse width) was focused onto a rotating tungsten target (Johnson-Matthey), and the energy was varied from 5 to 40 mJ/pulse. Laser-ablated tungsten atoms were co-deposited with H_2 in excess neon onto a 3.5 K CsI cryogenic window. FTIR spectra were recorded at 0.5 cm^{-1} resolution on with 0.1 cm^{-1} accuracy using an MCTB detector.

Density functional theoretical calculations of tungsten hydrides and tungsten hydride–hydrogen complexes were done for comparison. The Gaussian 98 program¹⁶ was employed to calculate the structures and frequencies of tungsten hydride molecules using the BPW91 functional,¹⁷ the 6-311++G(d,p) basis set for hydrogen, and SDD pseudopotential and basis for tungsten.^{18,19}

Figure 1 illustrates the W–H stretching region from the infrared spectrum of laser-ablated W atom reaction products with 4% H_2 in excess neon during condensation at 3.5 K. Stronger absorptions are observed at 1920.5, 1911.5, 1894.6, 1860.2, and 1831.9 cm^{-1} , and weaker peaks appear at 2004.4, 1953.8, 1927.5, 1080.3, and 840.7 cm^{-1} (latter two not shown). The weaker peaks in concert increase on annealing, decrease on photolysis, increase on further

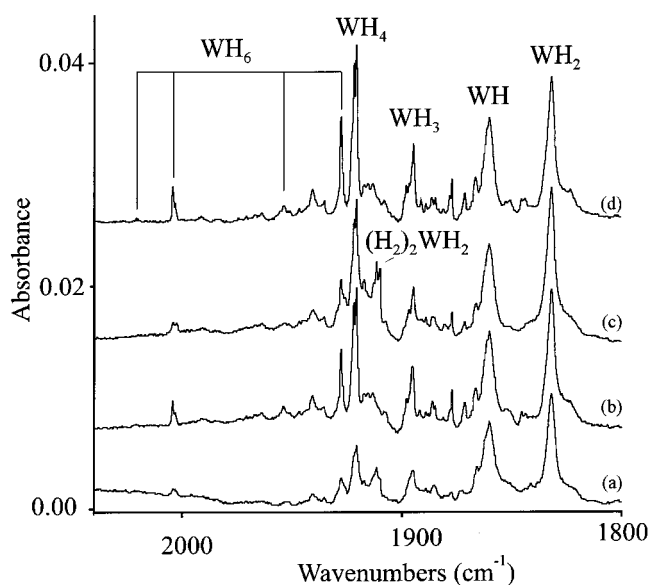


Figure 1. Infrared spectrum in the W–H stretching region for tungsten hydrides prepared by reacting laser-ablated W atoms and H_2 in excess neon during co-deposition at 3.5 K. (a) W and 4% H_2 co-deposited for 1 h in neon, (b) after annealing to 10 K, (c) after broadband photolysis for 15 min, and (d) after annealing to 11 K.

annealing, and acquire another weaker associated peak at 2021.2 cm^{-1} (Figure 1, parts b,c,d).

With the help of D_2 and HD substitution on the experimental frequencies and DFT calculations of isotopic frequencies for the minimum energy structures, the stronger above absorptions can be assigned, respectively, to WH_4 , $\text{WH}_2(\text{H}_2)_2$, WH_3 , WH and WH_2 . The details of these assignments and calculations will be reported in a longer paper.²⁰ The weaker six band group will be assigned here to WH_6 in the distorted C_{3v} prism structure based on agreement with frequencies computed by DFT.

The strongest four of the six new bands exhibit deuterium counterparts (Table 1) that define H/D isotopic frequency ratios 1.392, 1.393, 1.386, and 1.380, which are appropriate for W–H stretching and bending vibrations. Thus, the four highest frequencies are due to W–H stretching vibrations, and this provides diagnostic information for the new tungsten hydride structure.

First, the new tungsten hydride formed here with four W–H stretching frequencies cannot be octahedral WH_6 , which has one allowed triply degenerate W–H stretching mode. Second, the observed frequencies are not compatible with DFT predictions for the slightly higher energy C_{5v} parachute and umbrella structures and the C_{3v} hemisphere structure in terms of the number of observable (by calculated intensity) and relative positions of the W–H stretching modes.²⁰ However, the agreement between the four observed neon matrix W–H stretching frequencies and their relative intensities with those predicted by DFT for the distorted

* To whom correspondence should be addressed. E-mail: lsa@virginia.edu.

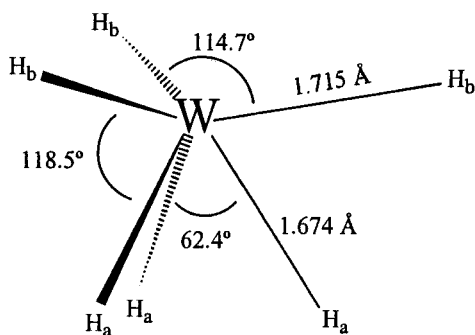
Table 1. Neon Matrix Observed and DFT Calculated Frequencies (cm^{-1}) for WH_6 in the Distorted Trigonal Prism Structure^a

observed			calculated
H ₂	D ₂	HD	H ₂ (mode, intensity, km/mol)
2021.2 (3) ^b			2059.3 (a ₁ , 45)
2004.4 (40)	1439.9	1432.5	2039.9 (e, 72 × 2)
1953.8 (12)		1952.6	1963.7 (a ₁ , 92)
1927.5 (100)	1384.1	1927.5	1949.8 (e, 141 × 2)
1080.3 (30)	779.2	797.9	1155.1 (a ₁ , 101)
			946.1 (e, 14 × 2)
840.7 (14)	609.1		894.0 (e, 60 × 2)
			805.8 (a ₂ , 0)
			758.6 (a ₁ , 10)
			709.5 (e, 9 × 2)

^a C_{3v} structure calculated at BPW91/6-311G(d,p)/SDD level: top three W–H bonds are 1.715 Å, H–W–H angles are 114.7°; bottom three W–H bonds are 1.674 Å, H–W–H angles are 62.4°. ¹A₁ ground-state WH_6 molecule. ^b Relative integrated band absorbances.

C_{3v} prism WH_6 structure (Table 1) is remarkable. Although frequencies calculated with the B3LYP functional²⁰ and at the all-electron SCF level are higher,³ the band profile and relative intensities are similar to those reported here for the BPW91 functional.

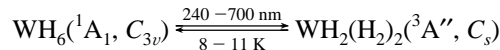
The distorted C_{3v} prism structure computed here and shown below for the ¹A₁ ground-state WH_6 molecule is almost the same as that calculated earlier.^{3–6} In addition, displacement coordinates show that the two highest W–H stretching frequencies are due mostly to the trigonal WH_3 subgroup with the shorter W–H_a bonds and acute H_a–W–H_a angles, and the next two frequencies are due to the WH_3 subgroup with the longer W–H_b bonds and obtuse H_b–W–H_b angles. Thus, each WH_3 subunit exhibits symmetric (a₁) and antisymmetric doubly degenerate (e) stretching modes, and vibrational coupling between these WH_3 subunits is minimal. The four W–H stretching modes are calculated 38, 35, 10, and 22 cm^{-1} (or 1.9, 1.7, 0.5, and 1.1%) too high by the BPW91 density functional, which is excellent agreement. However, the relative intensities do not fit quite as well, as the calculation overestimates the a₁ W–H stretching intensities. Bending and deformation modes are predicted 65 and 53 cm^{-1} (or 6.0 and 6.3%) too high with reasonable relative intensities. It is clearly more difficult to compute accurately lower-frequency bending vibrational motions.



Reaction with HD gives WH_3D_3 in four isotopic modifications, but the $\text{WD}_3(\text{short})\text{H}_3(\text{long})$ isotopomer with the lowest zero-point energy appears to be favored although weak bands are found for other isotopomers. The lowest-energy isotopomer exhibits the four HD frequencies listed in Table 1, which are near values for the $\text{WH}_3(\text{long})$ and $\text{WD}_3(\text{short})$ subunits of the WH_6 and WD_6 isotopic

molecules, respectively. The WH_3D_3 spectrum also supports the present assignments and substantiates this first experimental evidence for tungsten hexahydride.

It is interesting to note that broadband (240–700 nm) photolysis decreases WH_6 and produces the 26.0 kcal/mol higher energy high-spin $\text{WH}_2(\text{H}_2)_2$ complex, but further annealing allows the exothermic reformation of WH_6 . It appears that WH_6 is stable but facile and that H_2 molecules must be in a favored orientation for reaction with WH_2 to form WH_6 .



The present neon matrix experiments provide the proper dynamic conditions for reaction of laser-ablated W atoms and H_2 to form WH_2 during condensation in excess neon at 3.5 K. Some WH_2 reacts with more H_2 to form WH_4 and WH_6 . The latter reactions also occur on annealing the solid neon host to 8–11 K, which allows diffusion and spontaneous reaction of H_2 with WH_2 and WH_4 . The WH_6 formed here is identified by D_2 and HD isotopic substitution and by excellent agreement with frequencies computed by DFT for the distorted C_{3v} prism structure. Thus, structure determination is made by matching observed frequencies with frequencies calculated for a unique structure. Although there is evidence for higher hydride anion species in the solid state,²¹ WH_6 is the highest neutral hydride and the only neutral metal hexahydride to be observed experimentally.

Acknowledgment. We gratefully acknowledge support from NSF Grant CHE 00-78836.

References

- Gillespie, R. J.; Nyholm, R. S. *Q. Rev. Chem. Soc.* **1957**, *11*, 339.
- Kang, S. K.; Albright, T. A.; Eisenstein, P. *Inorg. Chem.* **1989**, *28*, 1611.
- Shen, M.; Schaefer, H. F., III.; Partridge, H. *J. Chem. Phys.* **1993**, *98*, 508.
- Kang, S. K.; Tang, H.; Albright, T. A. *J. Am. Chem. Soc.* **1993**, *115*, 1971.
- Tanpipat, N.; Baker, J. *J. Phys. Chem.* **1996**, *100*, 19818.
- Kaupp, M. *J. Am. Chem. Soc.* **1996**, *118*, 3018.
- Haaland, A.; Hammel, A.; Rypdal, K.; Volden, H. V. *J. Am. Chem. Soc.* **1990**, *112*, 4547.
- Pfennig, V.; Seppelt, K. *Science* **1996**, *271*, 626.
- Chertihin, G. V.; Andrews, L. *J. Am. Chem. Soc.* **1994**, *116*, 8322 (Ti + H_2).
- Chertihin, G. V.; Andrews, L. *J. Am. Chem. Soc.* **1995**, *117*, 6402 (Zr, Hf + H_2).
- Wang, X.; Andrews, L. *J. Am. Chem. Soc.* **2001**, *123*, 12899 (Au + H_2).
- Wang, X.; Andrews, L. *J. Phys. Chem. A* **2002**, *106*, 3706 (Rh + H_2).
- Burkholder, T. R.; Andrews, L. *J. Chem. Phys.* **1991**, *95*, 8697.
- Hassanzadeh, P.; Andrews, L. *J. Phys. Chem.* **1992**, *96*, 9177.
- Zhou, M.; Andrews, L. *J. Chem. Phys.* **1999**, *111*, 4230.
- Frisch, M. J.; Trucks, G. W.; Schlegel, H. B.; Scuseria, G. E.; Robb, M. A.; Cheeseman, J. R.; Zakrzewski, V. G.; Montgomery, J. A., Jr.; Stratmann, R. E.; Burant, J. C.; Dapprich, S.; Millam, J. M.; Daniels, A. D.; Kudin, K. N.; Strain, M. C.; Farkas, O.; Tomasi, J.; Barone, V.; Cossi, M.; Cammi, R.; Mennucci, B.; Pomelli, C.; Adamo, C.; Clifford, S.; Ochterski, J.; Petersson, G. A.; Ayala, P. Y.; Cui, Q.; Morokuma, K.; Malick, D. K.; Rabuck, A. D.; Raghavachari, K.; Foresman, J. B.; Cioslowski, J.; Ortiz, J. V.; Stefanov, B. B.; Liu, G.; Liashenko, A.; Piskorz, P.; Komaromi, I.; Gomperts, R.; Martin, R. L.; Fox, D. J.; Keith, T.; Al-Laham, M. A.; Peng, C. Y.; Nanayakkara, A.; Gonzalez, C.; Challacombe, M.; Gill, P. M. W.; Johnson, B. G.; Chen, W.; Wong, M. W.; Andres, J. L.; Head-Gordon, M.; Replogle, E. S.; Pople, J. A. *Gaussian 98*, revision A.6; Gaussian, Inc.: Pittsburgh, PA, 1998.
- (a) Becke, A. D. *J. Chem. Phys.* **1993**, *98*, 5648. (b) Lee, C.; Yang, W.; Parr, R. G. *Phys. Rev. B* **1988**, *37*, 785.
- (a) Krishnan, R.; Binkley, J. S.; Seeger, R.; Pople, J. A. *J. Chem. Phys.* **1980**, *72*, 650. (b) Frisch, M. J.; Pople, J. A.; Binkley, J. S. *J. Chem. Phys.* **1984**, *80*, 3265.
- Andrae, D.; Haussermann, U.; Dolg, M.; Stoll, H.; Preuss, H. *Theor. Chim. Acta* **1990**, *77*, 123.
- Wang, X.; Andrews, L. To be published.
- King, R. B. *Coord. Chem. Rev.* **2000**, *813*, 200.

JA020216W